Electronic Supplementary Information

Liquid ToF-SIMS revealing the oil, water, and surfactant interfacial evolution

Yanjie Shen[a], Jenn Yao[a, ‡], Jiyoung Son[a, ‡], Zihua Zhu[b], and Xiao-Ying Yu*[a]

[a] Energy and Environment Directorate, Pacific Northwest National Laboratory, Richland, WA 99354

[b] Environmental Molecular Sciences Laboratory, Pacific Northwest National Laboratory, Richland, WA 99354, USA

‡ Equal contributions

*Corresponding author: xiaoying.yu@pnnl.gov; Tel: 509-372-4524; Fax: 509-375-2999

Contents of this file

Contents

Additional experiment details, figures and tables are provided to support the content in the main text.

Experimental

Dry sample preparation and static ToF-SIMS data acquisition

The same procedure used in previous synthetic bilgewater generation studies have been used to prepare synthetic bilge samples.[1] To make synthetic shipboard emulsion droplets, a homogenizer (Omni Tissue Master, Model 125, 10 mm generator probe) was used to initially mix the solution for 2 min. at 35,000 rpm; and 10 min. sonication at 40 kHz was followed to make a consistent mixture. The prepared emulsion samples were deposited on a clean silicon (Si) wafer and dried using N_2 in a chemical hood. Once dried, the samples were loaded on the sample holder for analysis.

A ToF-SIMS V instrument (IONTOF GmbH, Münster, Germany) was used. The pressure of the main chamber was maintained at ~1×10^{-8} mbar during analysis. The primary ion beam was a 25 keV Bi_3^+ with 10 kHz pulse energy. The pulse width was 0.8 ns and the current was ~ 0.6 pA. SIMS spectra were acquired by rastering over an area of 500×500 μm^2 for 60 scans.[2]

Supplemental Figures

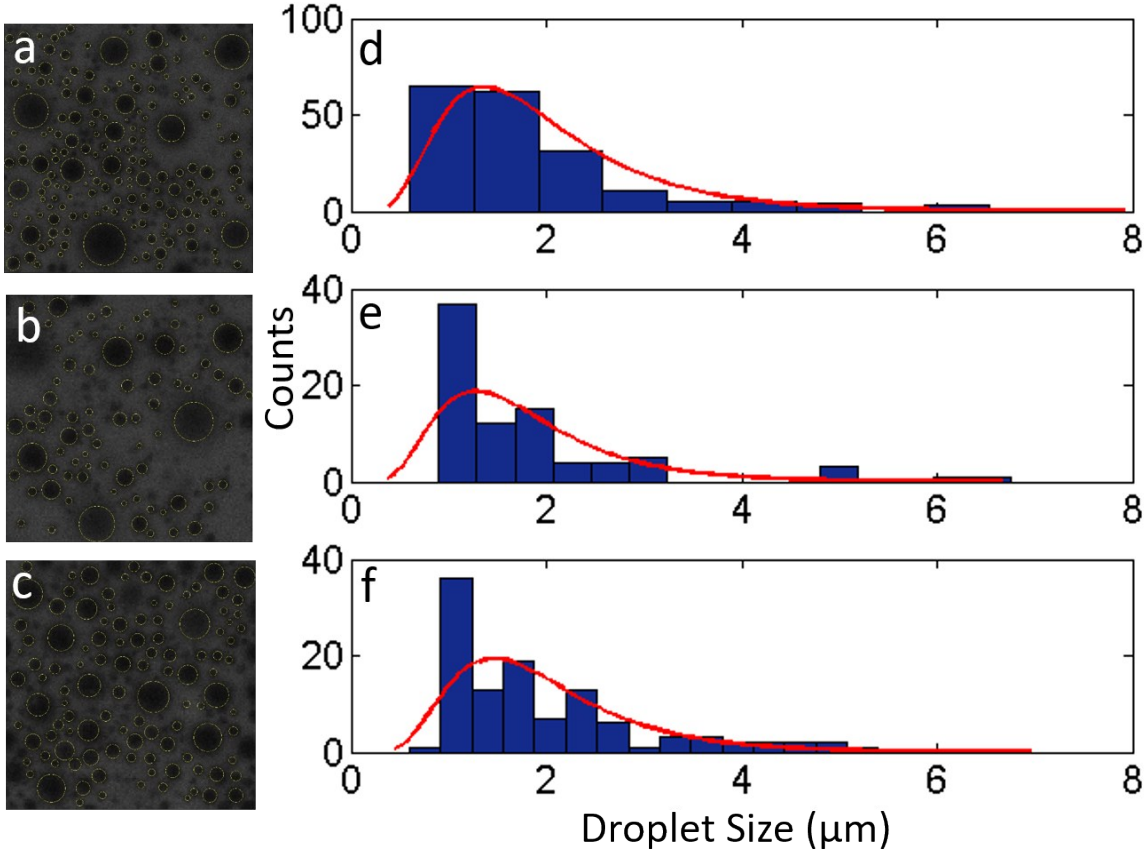

Figure S1a. Representative in situ SEM images and histograms showing fresh bilge DSD determination.

The droplet images were taken in three different SALVI devices shown in a, b, and c using in situ liquid SEM; and d, e, f were the corresponding histograms.

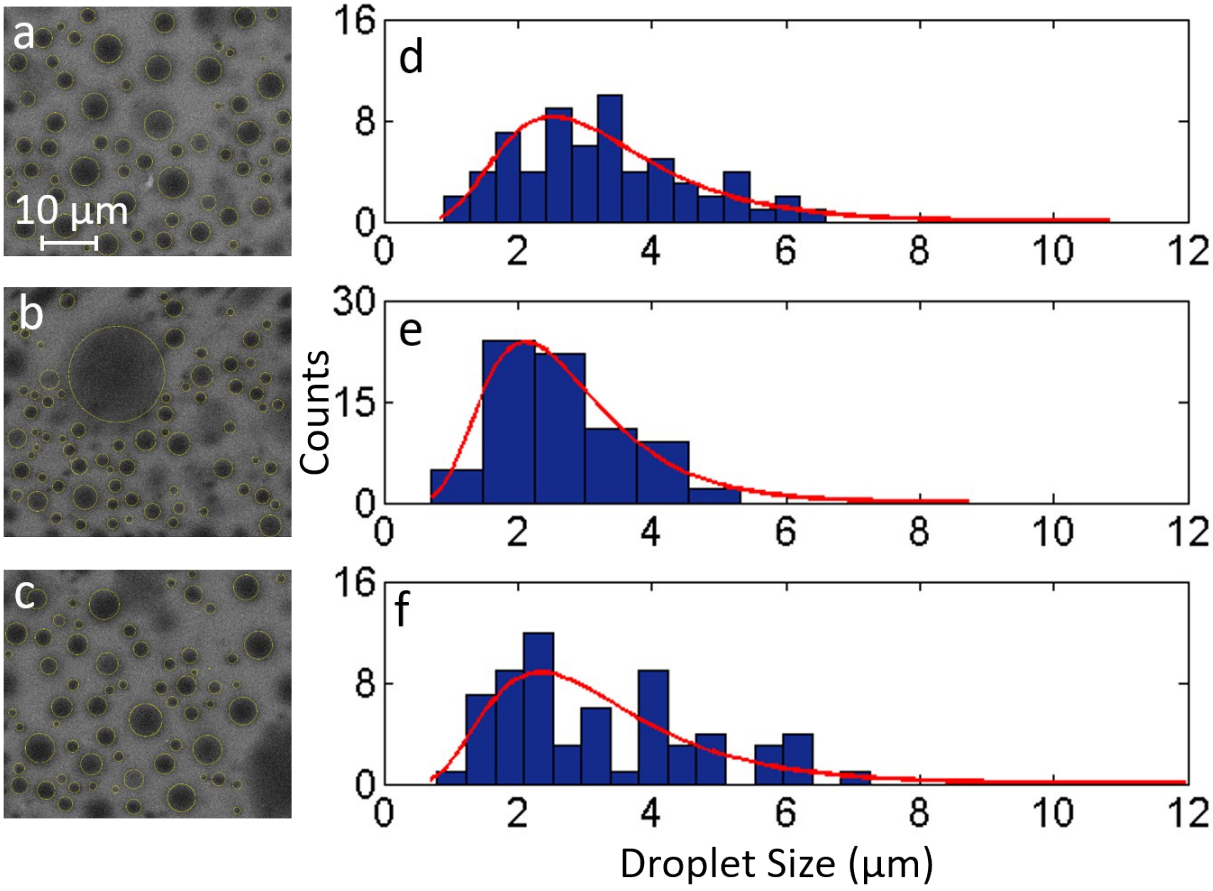

Figure S1b. Representative in situ liquid SEM images and histograms showing aged bilge DSD determination.

The droplet images were taken in three different SALVI devices shown in a, b, and c using in situ liquid SEM; and d, e, f were the corresponding histograms.

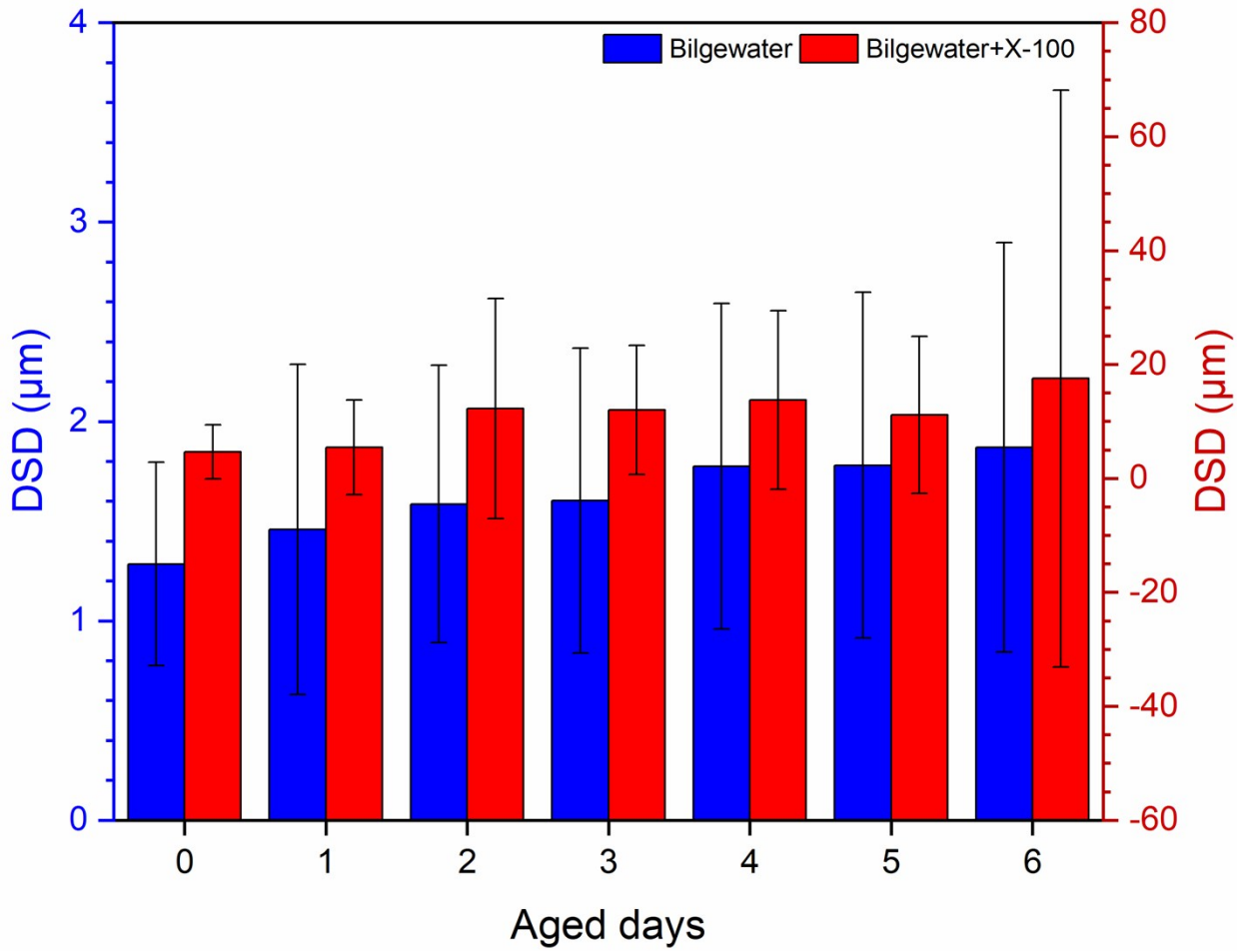

Figure S2a. Comparison of the DSD determination of bilgewater emulsions with X-100 added in six days at static conditions.

Error bars represent the standard deviation of six measurements.

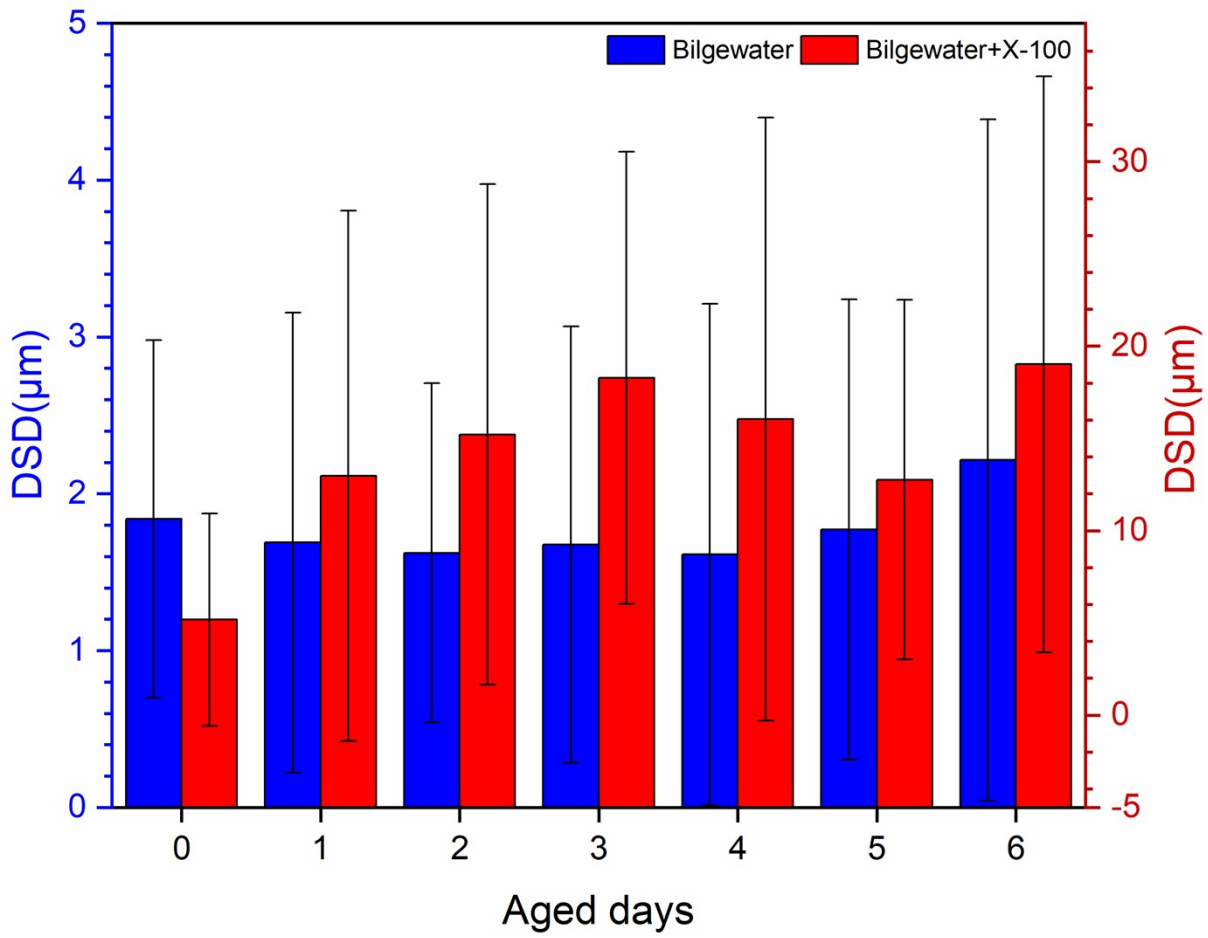

Figure S2b. Comparison of the DSD determination of bilgewater emulsions with X-100 added in six days at gently rocking conditions.

Error bars represent the standard deviation of six measurements. Figures S2a and 2b give the comparison of DSD determination of bilgewater emulsion with and without X-100 surfactant addition in six days at static and rocking conditions, respectively.

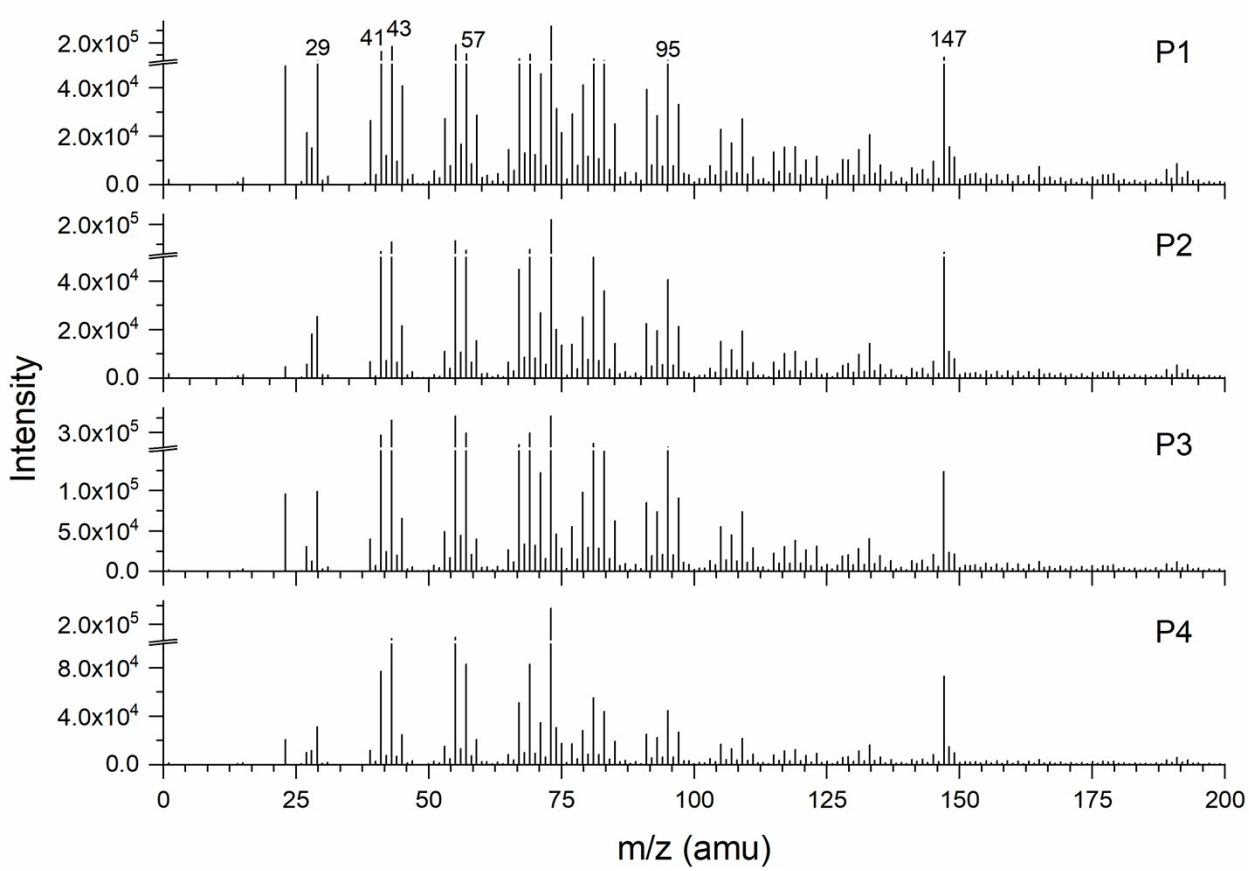

Figure S3a. Raw spectra showing reproducibility of liquid SIMS analysis of aged emulsion in the positive mode in the m/z$^+$ range 1 to 200.

P1, P2, P3, and P4 represent the first, second, third, and fourth positive ion mode spectral data acquired consecutively of the aged bilge sample inside a SALVI device.

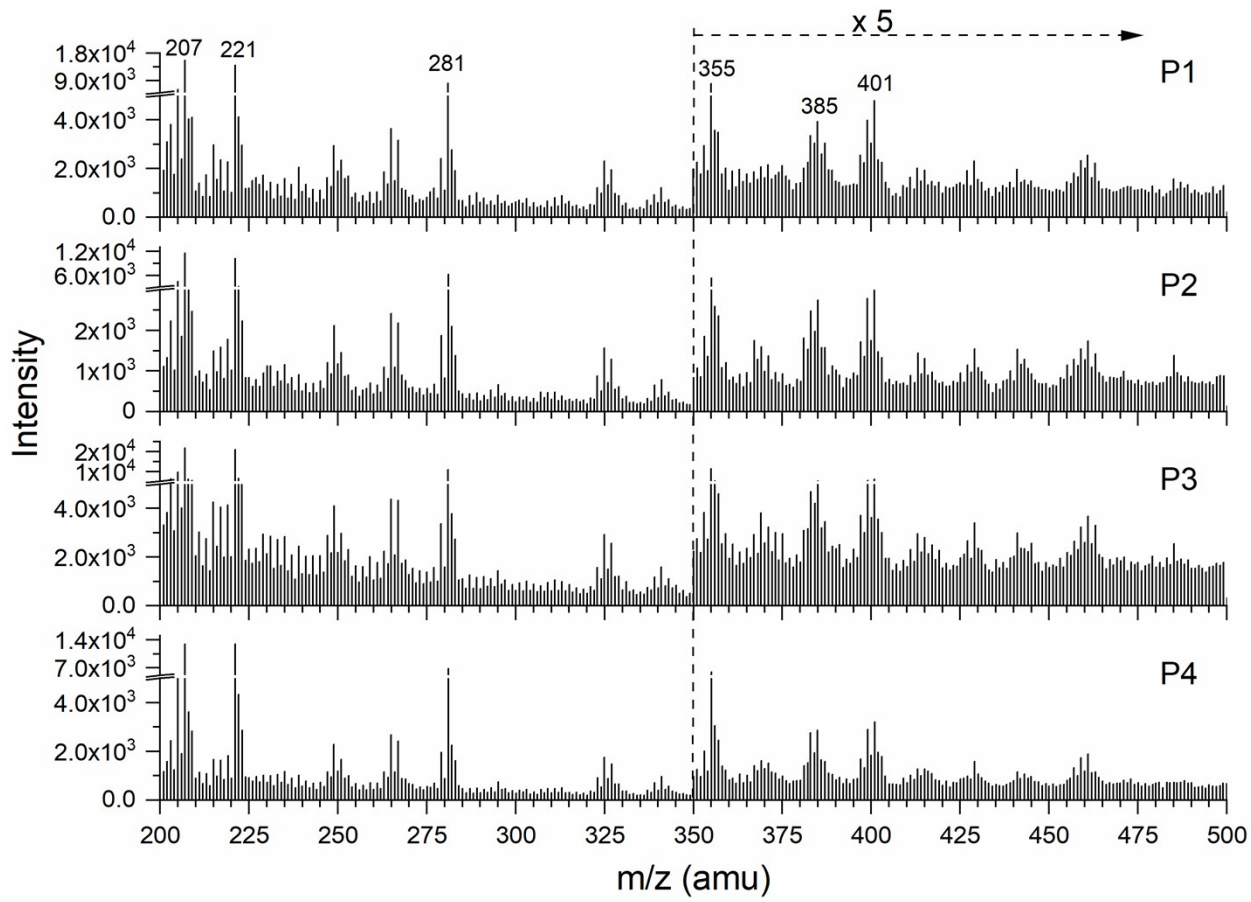

Figure S3b. Raw spectra showing reproducibility of liquid SIMS analysis of aged emulsion in the positive mode in the m/z$^+$ range of 200 to 500.

P1, P2, P3, and P4 represent the first, second, third, and fourth positive ion mode spectral data acquired consecutively of the aged bilge sample inside a SALVI device.

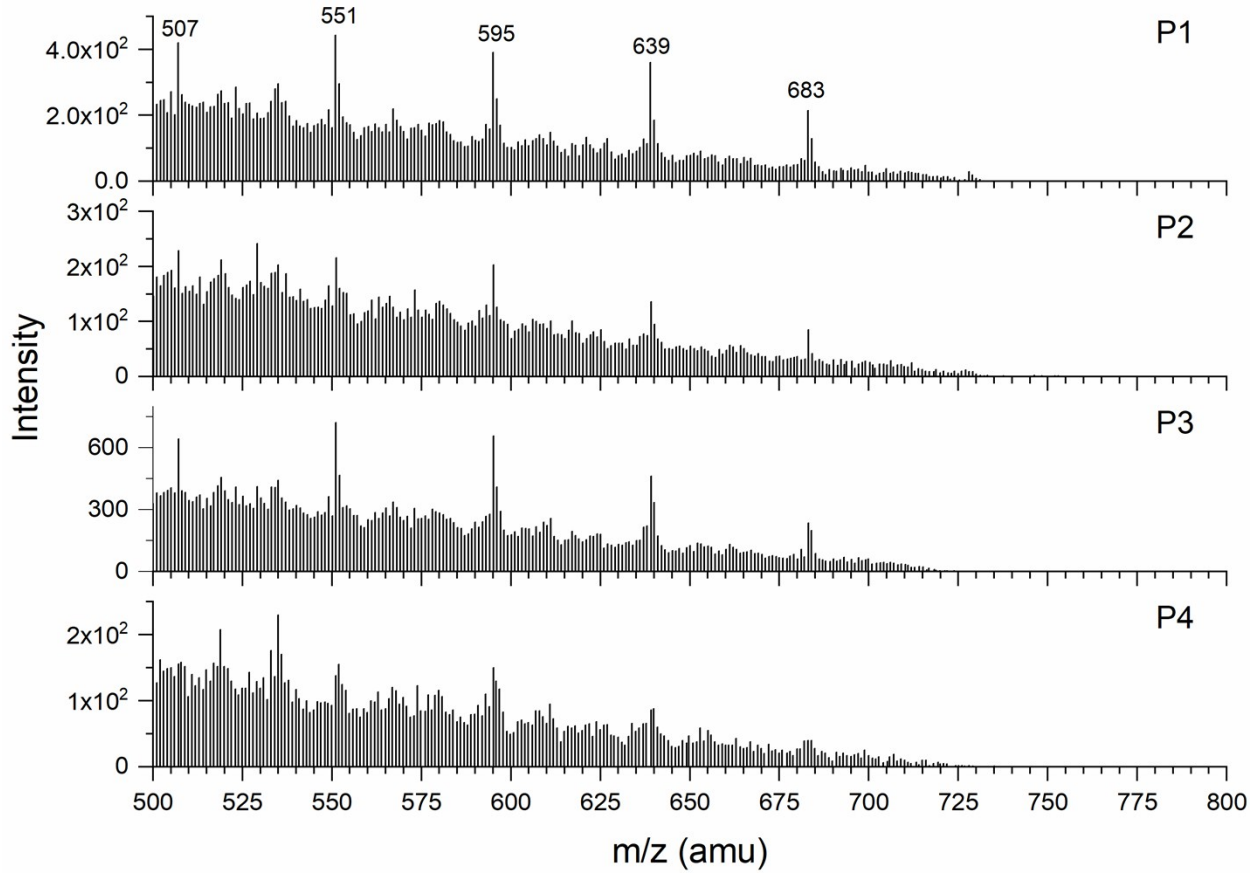

Figure S3c. Raw spectra showing reproducibility of liquid SIMS analysis of aged emulsion in the positive mode in the mass range of m/z^+ 500 to 800.

P1, P2, P3, and P4 represent the first, second, third, and fourth positive ion mode spectral data acquired consecutively of the aged bilge sample inside a SALVI device.

Overall, the liquid SIMS spectral comparison of the same samples in the positive ion mode show good reproducibility, thus giving assurance of data quality.

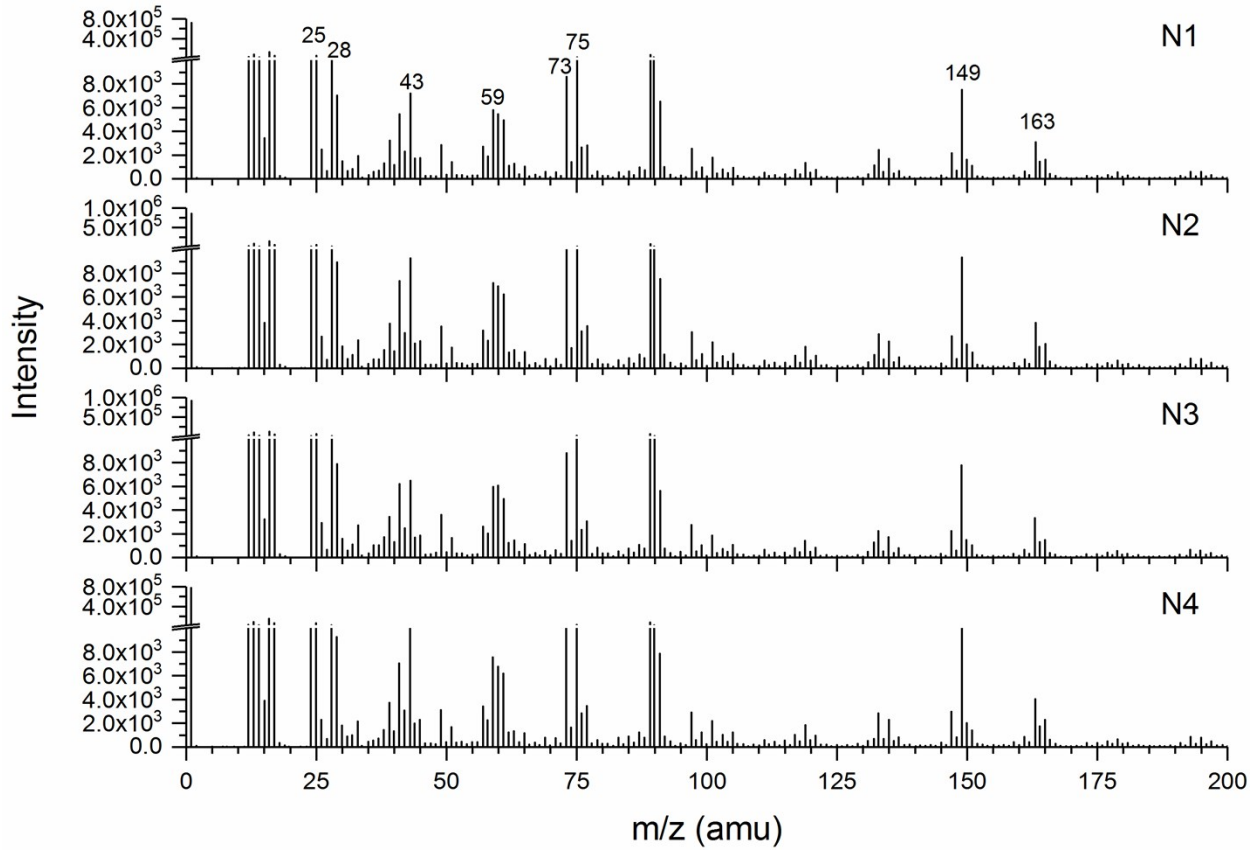

Figure S4a. Raw spectra showing reproducibility of liquid SIMS analysis of aged emulsion in the negative mode in the mass range of m/z$^-$ 0 to 200.

N1, N2, N3, and N4 represent the first, second, third, and fourth negative ion mode spectral data acquired consecutively of the aged bilge sample inside the SALVI device.

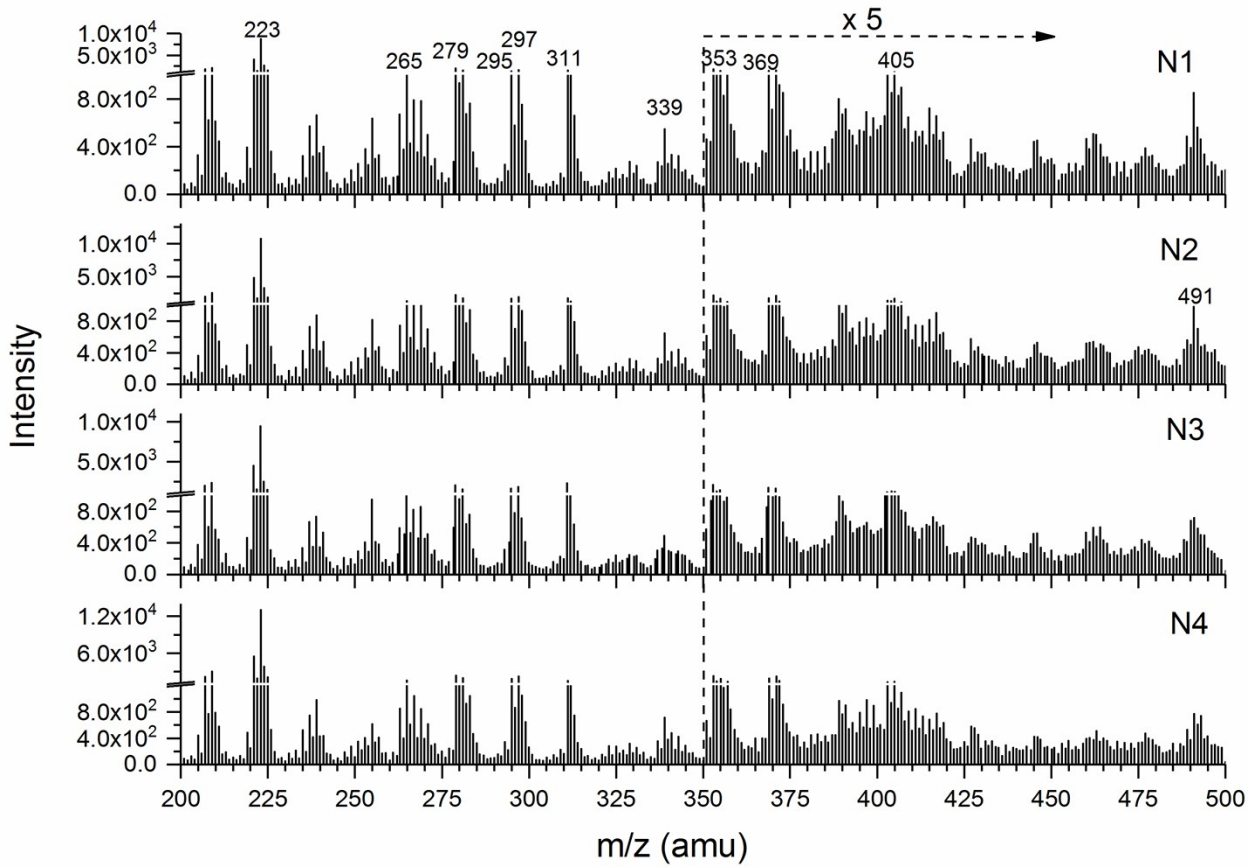

Figure S4b. Raw spectra showing reproducibility of liquid SIMS analysis of aged emulsion in the positive mode in the mass range of m/z$^-$ 200 to 500.

N1, N2, N3, and N4 represent the first, second, third, and fourth negative ion mode spectral data acquired consecutively of the aged bilge sample inside the SALVI device.

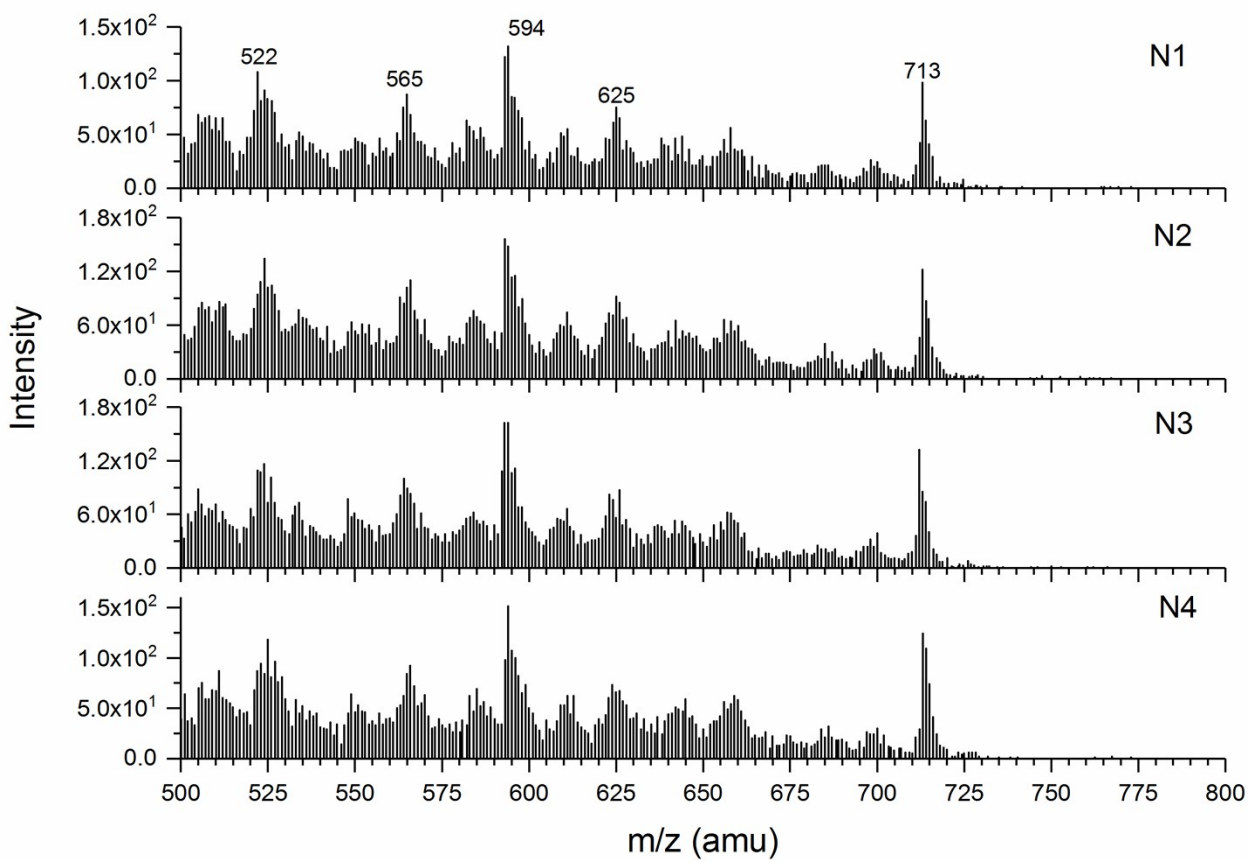

Figure S4c. Raw spectra showing reproducibility of liquid SIMS analysis of aged emulsion in the negative mode in the mass range of m/z$^-$ 500 to 800.

N1, N2, N3, and N4 represent the first, second, third, and fourth negative ion mode spectral data acquired consecutively of the aged bilge sample inside the SALVI device.

Overall, the liquid SIMS spectral comparison of the same samples in the negative ion mode show good reproducibility, thus giving us assurance of data quality.

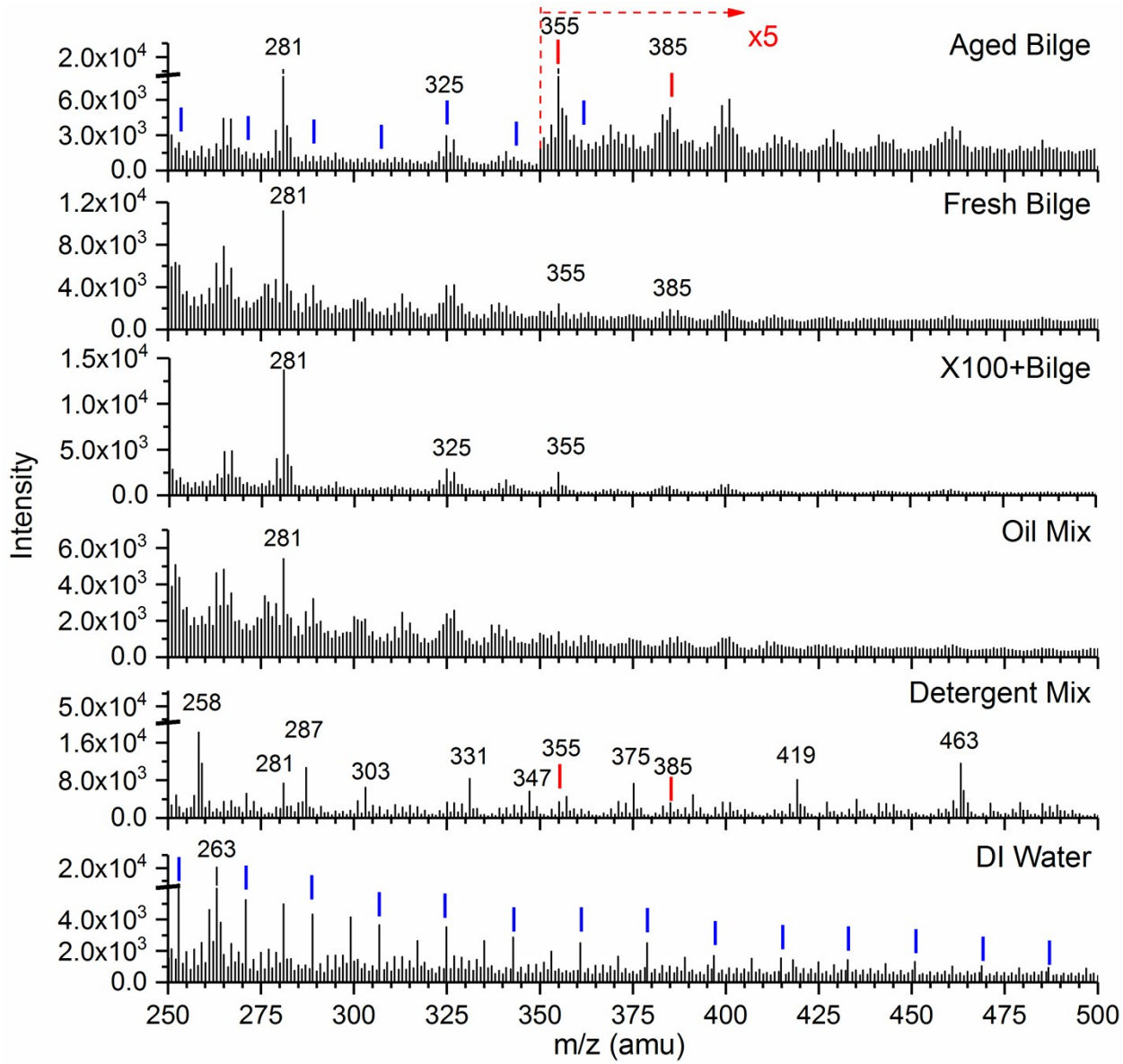

Figure S5a. Liquid SIMS spectral comparison of all samples in the positive ion mode in the mass range of m/z$^+$ 250 to 500.

Green, red, and blue bars represent oil, detergent, and water cluster peaks, respectively.

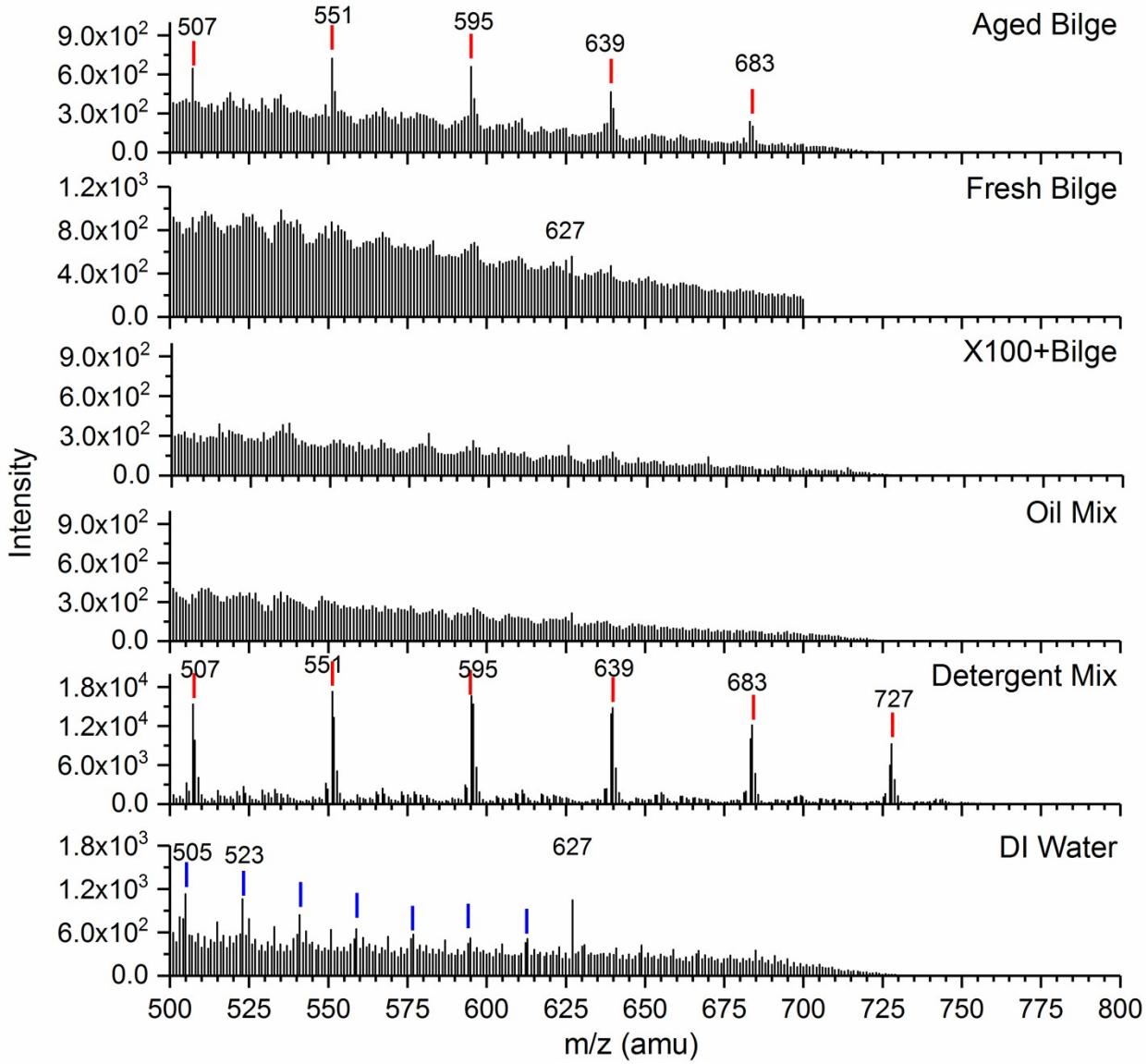

Figure S5b. Liquid SIMS spectral comparison of all samples in the positive ion mode in the mass range of m/z^+ 500 to 800.

Red and blue bars represent detergent and water cluster peaks, respectively.

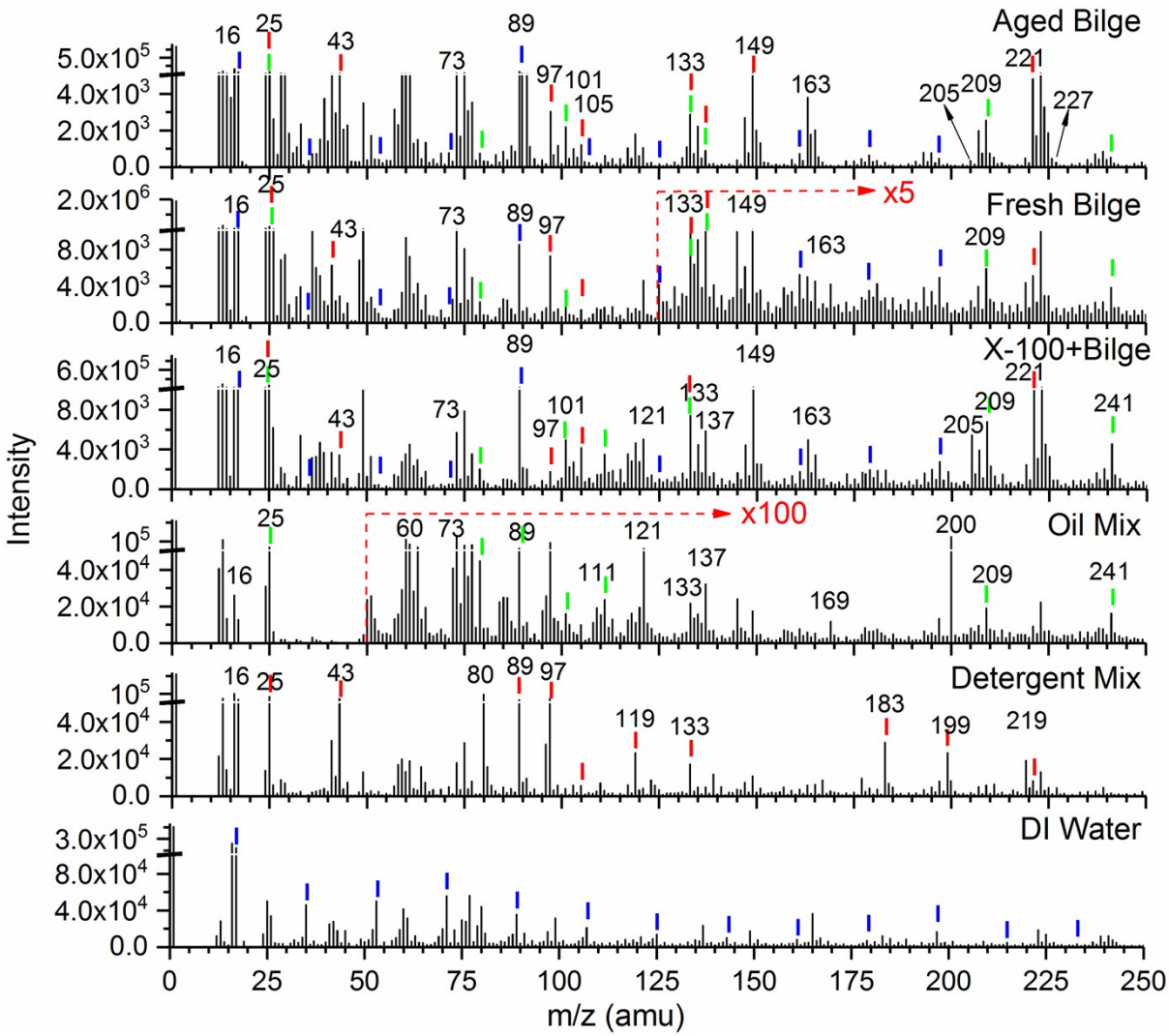

Figure S6a. Liquid SIMS spectral comparison of all samples in the negative ion mode in the mass range of m/z$^-$ 0 to 250.

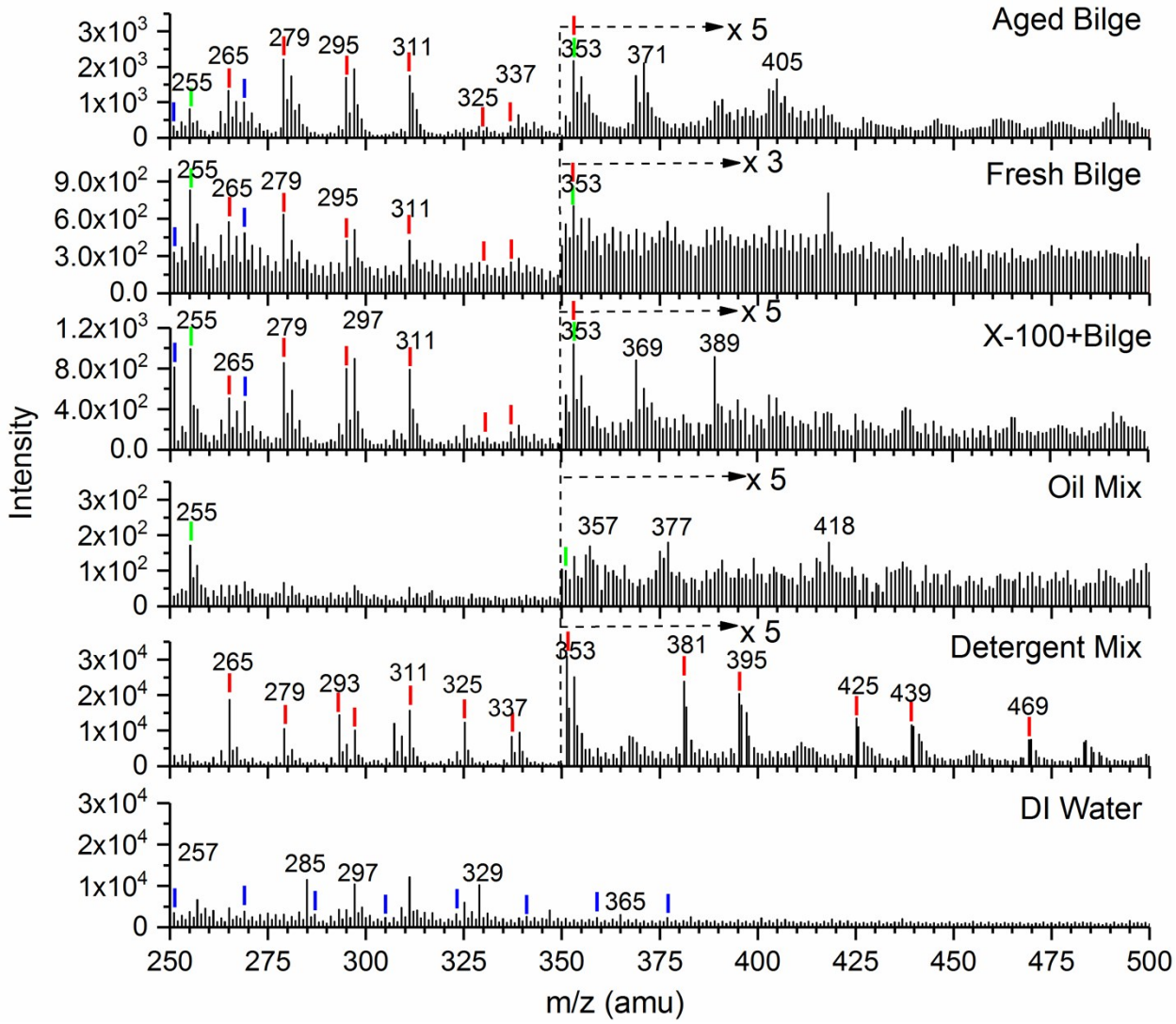

Figure S6b. Liquid SIMS spectral comparison of all samples in the negative ion mode in the mass range of m/z$^-$ 250 to 500.

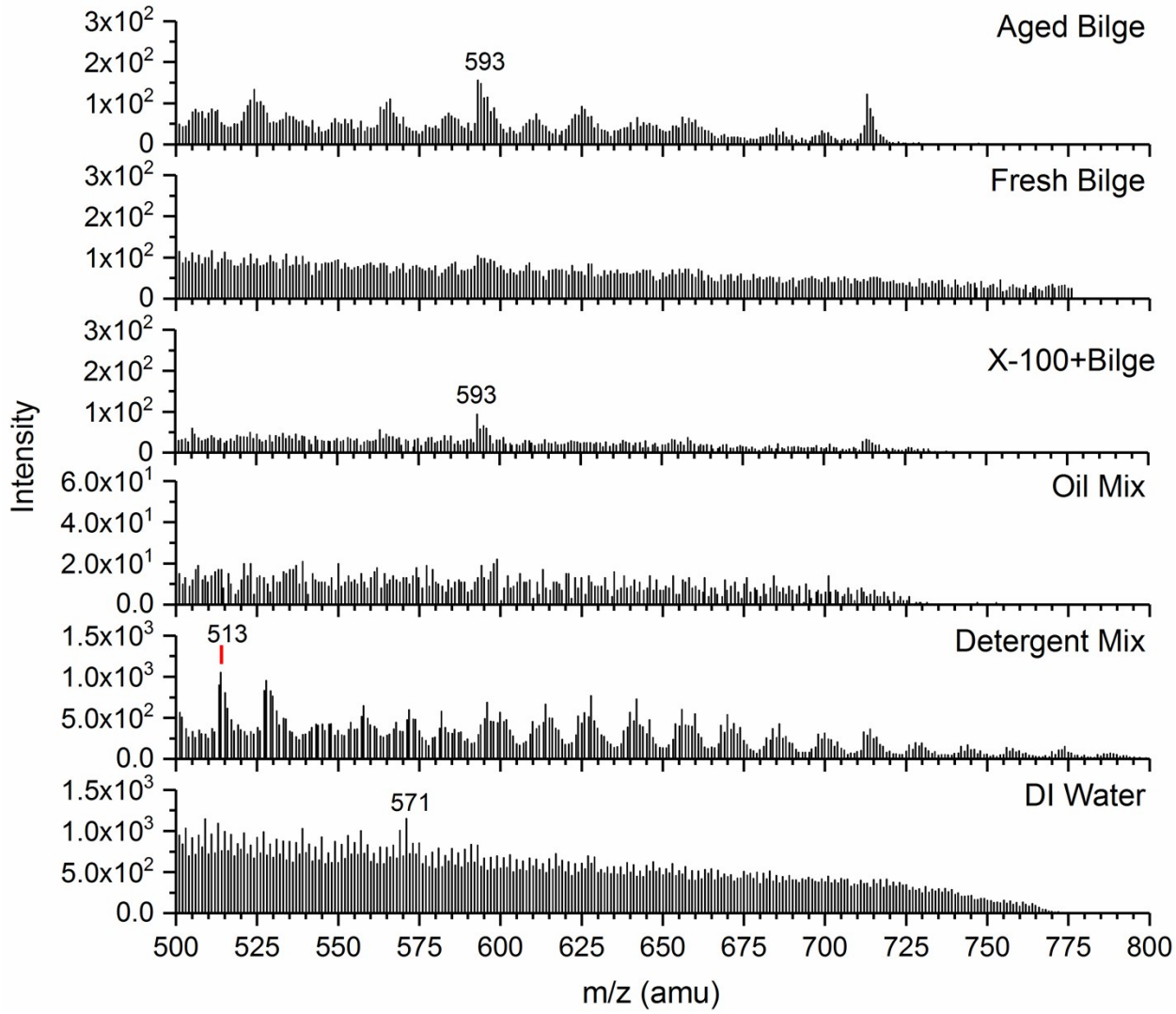

Figure S6c. Liquid SIMS spectral comparison of all samples in the negative ion mode in the mass range of m/z- 500 to 800.

Figures S6a, b, and c show liquid SIMS spectral comparison of the fresh bilge, aged bilge, X-100+fresh bilge, oil mix, detergent mix and DI water control in the negative ion mode. Oil components are observed in fresh bilge, aged bilge, and X-100+fresh bilge in the low mass range (i.e., m/z$^-$ 1-250). Many characteristic peaks are identified as hydrocarbon, such as m/z$^-$ 25 C_2H^-, 49 C_4H^-, 63 $C_5H_3^-$, and 79 $C_6H_7^-$. In the higher mass range (i.e., m/z$^-$ 250-500), the peaks that contribute to the bilge water spectra are mainly from detergent mix components, such as m/z$^-$ 279, 311, 325 $C_{18}H_{14}O_4P^-$, and 337 $C_{20}H_{33}O_4^-$. In the high mass rage (i.e., m/z$^-$ 500-800), oil peaks and detergent peaks are not significant contributors to the fresh bilge.

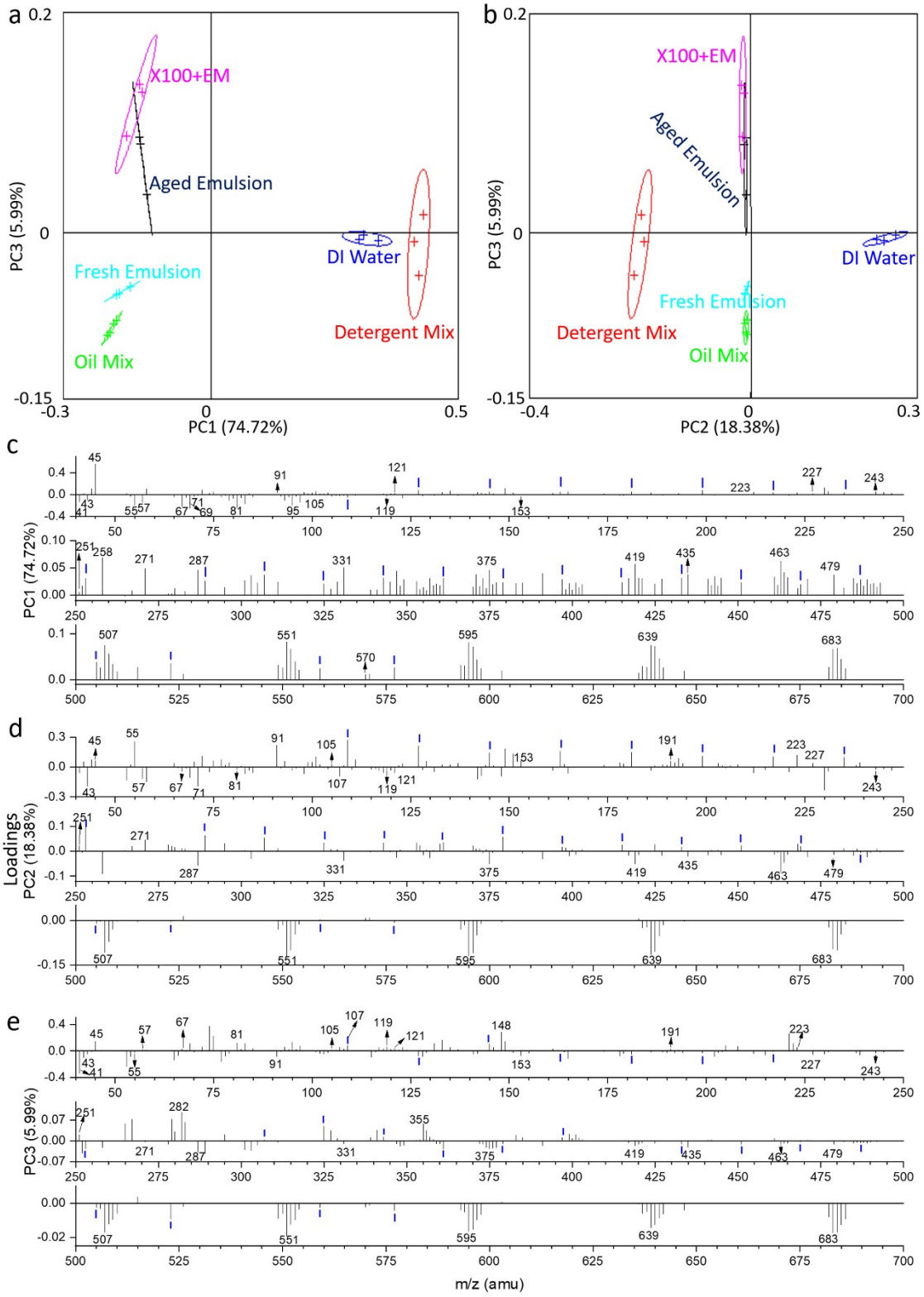

Figure S7. Spectral PCA of selected peaks of liquid samples in the positive mode: a) PC1 vs. PC3 scores plot; b) PC2 vs PC3 scores plot; and c) PC1, PC2 and PC3 loadings plots.

Figure S7 presents the scores plots of PC1 vs. PC3, PC2 vs. PC3, and principal components (PC1, PC2 and PC3) loadings plots in negative mode. In the positive mode, PC1, PC2 and PC3 explain 99.09% of all data. PC1 explains 74.72% of the data and mainly separates the DI water control and the detergent mix from the oil mix, fresh bilge, aged bilge and X-100+fresh bilge. PC2 explains 18.38% of the data and mainly separates the DI water from the aged bilge, fresh bilge, oil mix, and detergent mix. PC3 explains 5.99% of all data and mainly separates the DI water control, oil mix, and fresh bilge from aged bilge and X-100+fresh bilge.

Looking into the PC1 loadings, water cluster peaks are the main peaks that separate the detergent mix and DI water from the oil mix and fresh bilge. The identified detergent peaks are m/z$^+$ 45 $C_2H_5O^+$, 223 $C_{12}H_{15}O_4^+$, 227 $C_{13}H_{23}O_3^+$, 251 $C_{16}H_{21}O_2^+$, 271 $C_{17}H_{35}O_2^+$, and a series of fragments of TPGS including m/z$^+$ 243 $C_{10}H_{20}O_5Na^+$, 287 $C_{12}H_{24}O_6Na^+$, 331 $C_{14}H_{28}O_7Na^+$, 375 $C_{16}H_{32}O_8Na^+$, 419 $C_{18}H_{36}O_{10}Na^+$, 435 $C_{18}H_{36}O_{10}Na^+$, 463 $C_{20}H_{40}O_{10}Na^+$, 507 $C_{22}H_{44}O_{11}Na^+$, 551 $C_{24}H_{48}O_{12}Na^+$, 595 $C_{26}H_{52}O_{13}Na^+$, 639 $C_{28}H_{56}O_{14}Na^+$, and 683 $C_{30}H_{60}O_{15}Na^+$. The water cluster peaks are observed in DI water and detergent mix in a wide range. In PC1 negative, oil mix, fresh bilge, aged bilge, and X-100+fresh bilge share common peaks. Most of them are identified as hydrocarbon fragments, such as m/z$^+$ 41 $C_3H_5^+$, 43 $C_3H_7^+$, 55 $C_4H_7^+$, 57 $C_4H_9^+$, 67 $C_5H_7^+$, 69 $C_5H_9^+$, 71 $C_5H_{11}^+$, 81 $C_6H_9^+$, and 105 $C_8H_9^+$. In PC2 positive, DI water are separated from aged bilge, fresh bilge, X-100+fresh bilge, oil mix, and detergent mix. Aged bilge, fresh bilge, X-100+fresh bilge, oil mix and detergent mix share common components in the PC2 negative loadings, peaks that contribute to this commonality include hydrocarbon fragments such as m/z$^+$ 43 $C_3H_7^+$, 57 $C_3H_7^+$, 67 $C_5H_7^+$, 71 $C_5H_{11}^+$, 81 $C_6H_9^+$, or 121 $C_9H_{13}^+$ and detergent components such as m/z$^+$ 107 $C^4H^{11}O^{3+}$ and 119 $C_6H_{15}O_2^+$, and a series of fragments of TPGS. In addition, large water clusters, such as $(H_2O)_nH^+$, n=16-26 make important contributions to the formation of bilge emulsion. In PC3 positive loadings, aged bilge emulsion and X-100+fresh emulsion are separated from the oil mix, DI water, and fresh bilge emulsion; detergent mix have both positive and negative scores. In PC3 positive, aged bilge and X-100+fresh emulsion share some peaks, including hydrocarbon fragments such as m/z$^+$ 57 $C_4H_9^+$, 67 $C_5H_7^+$, 81 $C_6H_9^+$, 105 $C_8H_9^+$, and 121 $C_9H_{13}^+$ and detergent components such as m/z$^+$ 45 $C_2H_5O^+$, 107 $C_4H_{11}O_3^+$, 119 $C_6H_{15}O_2^+$, 191$C_{10}H_{23}O_3^+$, 223 $C_{12}H_{15}O_4^+$, and 251$C_{16}H_{27}O_2^+$. In PC3 negative, hydrocarbon fragments, such as m/z$^+$ 41$C_3H_5^+$, 43 $C_3H_7^+$, 55 $C_4H_7^+$, or 91 $C_7H_7^+$, detergent peaks, such as 153 $C_9H_{13}O_2^+$ and 227 $C_{13}H_{23}O_3^+$, and fragments of TPGS are the main peaks. PC3 separates the fresh and aged bilge emulsion, indicating the surface change of bilge emulsion over time.

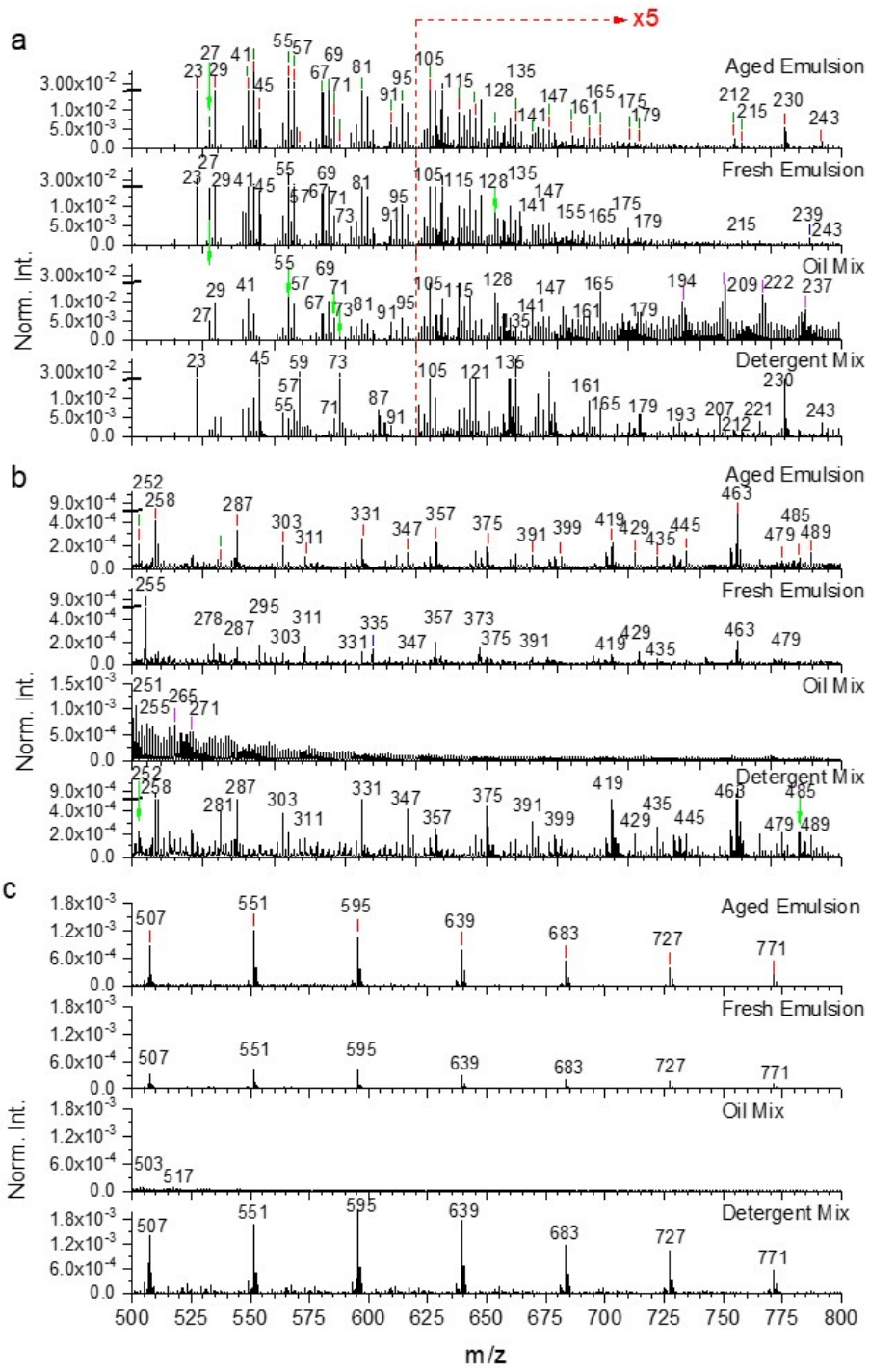

Figure S8 Static ToF-SIMS spectral comparison of synthetic bilgewater emulsion and key components: (a) m/z$^+$ 0-250, (b) 250-500 and (c) 500-800 in the positive ion mode. The green, red, blue and purple lines represent oil, detergent, newly formed and consumed components, respectively. (Adapted from Son et al. in Chemosphere).[2]

Figure S8 is adapted from our recent publication of static ToF-SIMS analysis of dried emulsion samples. When comparing the static and dynamic SIMS imaging, the oil components

appear in the fresh emulsion and persist in the aged emulsion, indicating they are at the droplet surface (Fig. S8a). The same is true with small detergent components (m/z^+ 0-250). However, the relative high mass detergent components (m/z^+ 250-500), such as m/z^+ 331 $C_{14}H_{28}O_7Na^+$, 347, 419 $C_{18}H_{36}O_9Na^+$, and 463 $C_{20}H_{40}O_{10}Na^+$ do not appear in the fresh and aged bilgewater surface in dynamic SIMS (Fig. S5a), different from the observation in the static SIMS (See Fig. S8b). The high mass detergent components (m/z^+ 500-800) were observed only in aged bilgewater in dynamic SIMS (Fig. S5b). In static SIMS, high mass detergent components are more abundant in aged emulsion droplets (Fig. S8c). Because only dried samples can be analyzed in static SIMS, liquid information is lost. In contrast, liquid ToF-SIMS shows that the surface composition is indeed different between fresh and aged emulsion droplets.

Supplemental tables

Table S1. Descriptions of bilge emulsion and main component mixtures for ToF-SIMS analysis

Sample name	Descriptions
Fresh bilge	The fresh bilge consisted of 10 mL oil mix and 1 mL detergent mix. The fresh emulsion was injected into the SALVI channel immediately for further analysis.
Aged bilge	The aged bilge was prepared using the same recipe of the fresh bilge emulsion and was allowed to stand for 24 hrs. before being introduced to the SALVI.
X100 + fresh bilge	The X100+fresh bilge sample consisted of 1 mL Triton X-100 and 10 mL fresh bilge. This sample was immediately analysis after preparation.
Oil mix	The oil mix sample consisted of 50% Diesel Fuel Marine (MIL-PRF-16884N), 25% 2190 TEP Stream Lube Oil (MIL-PRF-17331K), and 25% 9250 Diesel Lube Oil (MIL-PRF-9000L). Used as received.
Detergent mix	The detergent mix consisted of 50% Type 1 General Purpose Detergent MIL-D-16791G (1), 25% Commercial Detergent Tide Ultra (Liquid), and 25% Degreasing Solvent (Kustom 221, MIL-PRF-680C, Type III). Used as received.
DI water control	High purity DI water from the Millipore system

Liquid sample preparation was conducted in the fume hood to reduce possible air contamination. The bilge composition was the same as what recently published [1]. The liquid sample was injected into the SALVI channel immediately for further analysis. The preparation of DI water control followed existing procedures reported in our earlier publications [3, 4].

Table S2. Comparison of the droplet size distribution determination using in situ liquid SEM and optical microscopy

SEM					
Fresh			μm		
Image	1	2	3	Mean	Stdev*
Mean	2.03	1.83	1.20	1.69	0.43
Median	1.88	1.50	1.87	1.75	0.22
Variance	1.98	1.32	1.02	1.44	0.49
Mode	1.15	1.14	1.14	1.14	0.01
Aged 1 Day			μm		
Image	1	2	3	Mean	Stdev*
Mean	3.29	2.82	3.25	3.12	0.26
Median	3.17	2.38	2.85	2.80	0.40
Variance	1.68	4.81	2.28	2.92	1.66
Mode	2.68	2.33	2.45	2.49	0.18

* The reported uncertainties are purely from statistical errors and they do not include the optical microscopy measurement limitation.

Table S3. The bilgewater droplet size distribution changes with and without X-100 addition over six days determined by optical microscopy

Bilgewater	Static conditions						
Droplet Age Day	0	1	2	3	4	5	6
Average (μm)	1.29	1.46	1.59	1.60	1.78	1.78	1.87
Variance (μm)	0.51	0.83	0.70	0.76	0.82	0.87	1.03
Median (μm)	1.17	1.23	1.39	1.37	1.58	1.54	1.58
Bilgewater+X-100	Static conditions						
Droplet Age Day	0	1	2	3	4	5	6
Average (μm)	4.66	5.47	12.26	12.01	13.74	11.15	17.54
Variance (μm)	4.72	8.31	19.29	11.29	15.69	13.79	50.64
Median (μm)	3.13	3.08	2.99	7.41	8.91	4.72	12.25
Bilgewater	Rocking conditions						
Droplet Age Day	0	1	2	3	4	5	6
Average (μm)	1.84	1.69	1.62	1.68	1.61	1.77	2.22
Variance (μm)	1.14	1.47	1.08	1.39	1.60	1.47	2.17
Median (μm)	1.41	1.24	1.27	1.22	1.24	1.25	1.49
Bilgewater+X-100	Rocking conditions						
Droplet Age Day	0	1	2	3	4	5	6
Average (μm)	5.17	12.98	15.22	18.28	16.05	12.77	19.01
Variance (μm)	5.76	14.37	13.56	12.26	16.34	9.75	15.60
Median (μm)	2.95	7.03	11.10	15.11	8.96	10.78	13.44

Table S3 gives a general statistical summary of the droplet size evolution of bilgewater emulsions with and without X-100 enhancement over six days.

There is some discrepancy between in situ SEM and optical microscopy measurements, because in situ SEM uses much higher magnification (i.e., × 5000 times). For micrometer-sized droplets, the optical microscope we have only offers up to 1000 times magnification. In addition, analysis depth is different. The SEM analysis volume is a sphere of approximately 1 μm in diameter, whereas optical microscopy would offer larger depth. The latter may result in some interferences in droplet counting. However, optical microscopy is faster to perform compared to in situ SEM at present. Because in situ SEM is a new technique and a feed-through is not available for this experiment.

Table S4. Possible peak identification in the positive mode

m/z^+_{exact}	$m/z^+_{obs.}$	Formula	Chemical description	Notes	References
22.990	23	Na^+	Inorganic ion		[f]
27.023	27	$C_2H_3^+$	Hydrocarbon		[f]
29.039	29	$C_2H_5^+$	Hydrocarbon		[f]
41.039	41	$C_3H_5^+$	Hydrocarbon		[f]
43.055	43	$C_3H_7^+$	Hydrocarbon		[f]
45.034	45	$C_2H_5O^+$	Alcohols or carbonyl		[f]
55.055	55	$C_4H_7^+$	Hydrocarbon		[f]
57.070	57	$C_4H_9^+$	Hydrocarbon		[f]
59.050	59	$C_3H_7O^+$	Alcohols or carbonyl		[f]
67.055	67	$C_5H_7^+$	Hydrocarbon		[f]
69.070	69	$C_5H_9^+$	Hydrocarbon		[f]
71.086	71	$C_5H_{11}^+$	Hydrocarbon		[f]
81.070	81	$C_6H_9^+$	Hydrocarbon		[f]
91.055	91	$C_7H_7^+$	Hydrocarbon		[f]
	95		--[a]	[b]	
105.070	105	$C_8H_9^+$	Hydrocarbon		[f]
107.071	107	$C_4H_{11}O_3^+$	Polyethylene glycol	[e]	[g]
	115		--[a]	[b]	
119.107	119	$C_6H_{15}O_2^+$	Ethanol, 2-butoxy-	[e]	[g]
121.102	121	$C_9H_{13}^+$	Hydrocarbon		[f]
	128		--[a]	[b]	
	135		--[a]	[b, c]	
153.092	153	$C_9H_{13}O_2^+$	1-Phenoxypropan-2-ol		[g]
	161		--[a]	[b, c]	
	175		--[a]	[b, c]	
	179		--[a]	[b, c]	
191.165	191	$C_{10}H_{23}O_3^+$	2-Propanol, 1-(2-butoxy-1-	[e]	[g]
	194		--[a]	[b]	
	212		--[a]	[c]	
	221		--[a]	[c]	
	222		--[a]	[b]	
223.097	223	$C_{12}H_{15}O_4^+$	Diethyl phthalate		
227.165	227	$C_{13}H_{23}O_3^+$	Cyclopentaneacetic acid, 3-oxo-2-pentyl-,methyl ester	[e]	[g]
	230		--[a]	[c]	
243.121	243	$C_{10}H_{20}O_5Na^+$	Fragment of TPGS	[d]	[i]
251.201	251	$C_{16}H_{27}O_2^+$	Triton X-41	[e]	[g]
	252		--[a]	[c]	
	258		--[a]	[c]	
271.264	271	$C_{17}H_{35}O_2^+$	Hexadecanoic acid, methyl ester	[e]	[g]

m/z^+_{exact}	$m/z^+_{obs.}$	Formula	Chemical description	Notes	References
	278		--[a]	[c]	
287.147	287	$C_{12}H_{24}O_6Na^+$	Fragment of TPGS	[d]	i
	295		--[a]	[c]	
	303		--[a]	[c]	
	311		--[a]	[c]	
331.173	331	$C_{14}H_{28}O_7Na^+$	Fragment of TPGS	[d]	h
	347		--[a]	[c]	
	357		--[a]	[c]	
	373		--[a]	[c]	
375.199	375	$C_{16}H_{32}O_8Na^+$	Fragment of TPGS	[d]	h
	391		--[a]	[c]	
419.225	419	$C_{18}H_{36}O_9Na^+$	Fragment of TPGS	[d]	h
435.220	435	$C_{18}H_{36}O_{10}Na^+$	Fragment of TPGS	[d]	h
	445		--[a]	[c]	
463.251	463	$C_{20}H_{40}O_{10}Na^+$	Fragment of TPGS	[d]	h
479.246	479	$C_{20}H_{40}O_{11}Na^+$	Fragment of TPGS	[d]	h
	489		--[a]	[c]	
507.278	507	$C_{22}H_{44}O_{11}Na^+$	Fragment of TPGS	[d]	h
551.304	551	$C_{24}H_{48}O_{12}Na^+$	Fragment of TPGS	[d]	h
570.377	570	$C_{31}H_{54}O_9^+$	Alkyl aryl polyether alcohol	[e]	g
595.330	595	$C_{26}H_{52}O_{13}Na^+$	Fragment of TPGS	[d]	h
639.356	639	$C_{28}H_{56}O_{14}Na^+$	Fragment of TPGS	[d]	h
683.382	683	$C_{30}H_{60}O_{15}Na^+$	Fragment of TPGS	[d]	h
727.409	727	$C_{32}H_{64}O_{16}Na^+$	Fragment of TPGS	[d]	h
771.435	771	$C_{34}H_{68}O_{17}Na^+$	Fragment of TPGS	[d]	h

[a.] not assigned; [b.] Detergent component; [c.] Oil component; [d.] Fragment of D-α-tocopheryl polyethylene glycol succinate (TPGS);[5] [e.] Based on the molecular weight; [f.] Reference is from Li et al.;[6] [g.] Reference is from PubChem database. When looking for information of a chemical, the CASRN is used to locate the exact chemical and its associated information;[7] [h.] Reference is from Wei et al.[8] [i.] Reference is from Son et al.[2]

Table S4 gives more detailed peak identification information in the positive ion mode. PDMS interference peaks were not included.

Table S5. Possible peak identification in the negative mode

m/z^-_{exact}	$m/z^-_{obs.}$	Formula	Chemical description	Notes	References
13.008	13	CH^-	Hydrocarbon		[e]
25.008	25	C_2H^-	Hydrocarbon		[e]
	43		--[a]	[b]	
49.008	49	C_4H^-	Hydrocarbon		[e]
63.023	63	$C_5H_3^-$	Hydrocarbon		[e]
79.055	79	$C_6H_7^-$	Hydrocarbon		[e]
96.960	97	HSO_4^-	Inorganic Ion		[e]
101.060	101	$C_5H_9O_2^-$	Fatty acid	[d]	[f]
105.055	105	$C_4H_9O_3^-$	Polyethylene glycol	[d]	[f]
	111		--[a]	[c]	
115.076	115	$C_6H_{11}O_2^-$	Fatty acid	[e]	[f]
	119		--[a]	[b]	
	133		--[a]	[b, c]	
	137		--[a]	[b, c]	
205.217	205	$C_{12}H_{29}O_2^-$	Polyethylene glycol	[d]	[f]
	219		--[a]	[b]	
221.081	221	$C_{12}H_{13}O_4^-$	Diethyl Phthalate	[d]	[f]
227.201	227	$C_{14}H_{27}O_2^-$	Tetradecanoic acid	[d]	[f]
255.232	255	$C_{16}H_{31}O_2^-$	n-Hexadecanoic acid	[d]	[f]
265.157	265	$C_{12}H_{26}O_4P^-$	Tributyl phosphate	[d]	[f]
269.248	269	$C_{17}H_{33}O_2^-$	Fatty acid		[g]
277.144	277	$C_{16}H_{21}O_4^-$	DBP	[d]	[f]
	293		--[a]	[b]	
	297		--[a]	[b, c]	
	307		--[a]	[b]	
	311		--[a]	[b]	
325.063	325	$C_{18}H_{14}O_4P^-$	Triphenyl phosphate		[f]
337.238	337	$C_{20}H_{33}O_4^-$	Triton X-41		[f]
	351		--[a]	[b]	
	353		--[a]	[b, c]	
	381		--[a]	[b]	
	395		--[a]	[b]	
425.290	425	$C_{24}H_{41}O_6^-$	Triton X-45		[f]
	439		--[a]	[b]	
	469		--[a]	[b]	
	483		--[a]	[b]	
513.343	513	$C_{28}H_{49}O_8^-$	Triton X-114		[f]

[a.] not assigned; [b.] Detergent component; [c.] Oil component; [d.] Based on the molecular weight; [e.] Reference is from Li et al.;[6] [f.] Reference is from PubChem database. When looking for information of a chemical, the CASRN is used to locate the exact chemical and its associated information;[7] [g.] Reference is from Leefmann et al.[9]

Table S5 gives more detailed peak identification information in the negative ion mode. PDMS interference peaks were not included.

Reference

1. J. Church, D. M. Paynter and W. H. Lee, *Langmuir*, 2017, **33**, 9731-9739.
2. J. Son, Y. Shen, J. Yao, D. Paynter and X.-Y. Yu, *Chemosphere*, 2019, **236**, 124345.
3. Y. Fu, Y. Zhang, F. Zhang, J. Chen, Z. Zhu and X.-Y. Yu, *Atmos. Environ.*, 2018, **191**, 36-45.
4. X. Sui, Y. Zhou, F. Zhang, Y. Zhang, J. Chen, Z. Zhu and X.-Y. Yu, *Surf. Interf. Anal.*, 2018, **50**, 927-938.
5. J. Zhang, Q. Xue, X. Pan, Y. Jin, W. Lu, D. Ding and Q. Guo, *Chemical Engineering Journal*, 2017, **307**, 643-649.
6. W. Li, H. Li, J. Li, X. Cheng, Z. Zhang, F. Chai, H. Zhang, T. Yang, P. Duan, D. Lu and Y. Chen, *J Environ Sci (China)*, 2018, **69**, 61-76.
7. NIH, PubChem, https://pubchem.ncbi.nlm.nih.gov/, Accessed April 15, 2019, 2019.
8. J. Wei, A. Bristow, E. McBride, D. Kilgour and P. B. O'Connor, *Analytical Chemistry*, 2014, **86**, 1567-1574.
9. T. Leefmann, C. Heim, A. Kryvenda, S. Siljeström, P. Sjövall and V. Thiel, *Organic Geochemistry*, 2013, **57**, 23-33.